HYPERSPECTRAL IMAGE DENOISING VIA SPECTRAL AND SPATIAL LOW-RANK APPROXIMATION

Yi Chang, Luxin Yan, and Sheng Zhong

{yichang, luxinyan, zhongsheng}@hust.edu.cn
School of Automation, Huazhong University of Science and Technology, China

ABSTRACT

Hyperspectral images (HSI) unavoidably suffer from degradations such as random noise, due to photon effects, calibration error, and so on. Most of existing HSI denoising methods focus on utilizing the spectral correlation or the spatial non-local self-similarity individually. In this paper, we propose an unified low-rank recovery framework for HSI denoising, in which taking both the underlying characteristics of high correlation across spectra and non-local self-similarity over the space cubic of HSI into consideration simultaneously. Our work rely on a basic observation that both the multiple spectral bands and similar spatial structures are lying on low-rank subspaces and can facilitate to remove the noise jointly. Experimental results on both simulated and real HSI demonstrate that the proposed method can significantly outperform the state-of-the-art methods on several datasets in terms of both visual and quantitative assessment.

***Index Terms*—** Hyperspectral imaging, denoising, low-rank.

1. INTRODUCTION

Most HSI classification/recognition algorithms assume that the input HSI is of scene content that is clear and visible. However, HSI often suffers from random noise in individual bands, which badly limits the subsequent processing. Therefore, it is natural for us to remove the noise as an important preprocessing procedure.

As an classical yet hot research field, a variety of HSI denoising methods have been proposed for the restoration of HSIs. The HSI denoising methods have been classified into different categories. In this work, we classify the HSI denoising methods into two categories according to the utilization information: spectral methods [1, 2, 3, 4, 5, 6] and spatial non-local self-similarity methods [7, 8, 9, 10]. The first kind of methods mainly rely on the high spectral correlation in HSI. In [1], by lexicographically ordering the 3D cube into a 2D matrix, the authors proposed a low-rank matrix restoration method for mixed noise removal in HSI. Further, Lu *et al*. [6] incorporated extra sparse constraint on the spectral information. Although these low-rank matrix recovery methods have achieved impressive result in HSI denoising, they have not fully exploit the abundantly spatial information in HSI.

Thanks to National Natural Science Foundation of China under Grant No. 61571207 for funding.

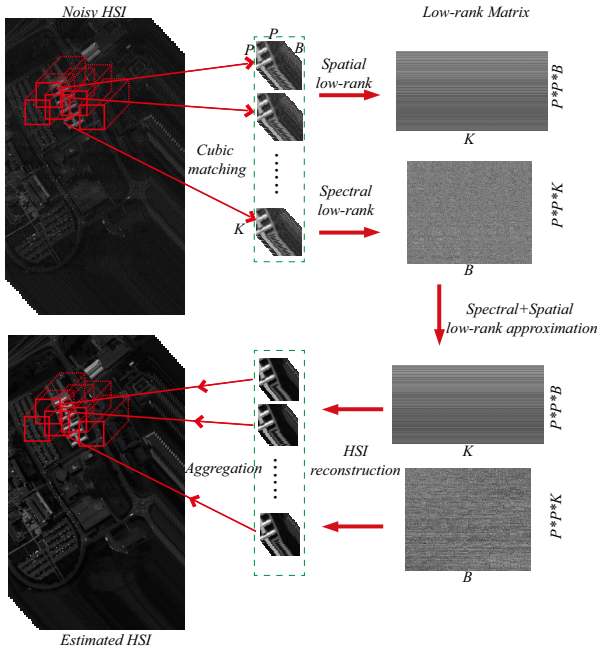

Fig. 1. Flowchart of the proposed HSI denoising algorithm. We construct the low-rank matrix across spectral dimension and spatial non-local similarity dimension, respectively.

Another research line follows the non-local self-similarity perspective which has been used widely in single image denoising. The well-known BM3D method was also naturally extended into BM4D [10] for volumetric data restoration. In [7], the authors proposed a tensor dictionary learning model via grouping similar patches for MSI denoising with hard constraints on the rank of the core tensor. However, they have neglected the exclusively spectral correlation property in HSI.

In this work, a unified low-rank approach is proposed to simultaneously involve the spatial and spectral structure information to obtain a complete representation of HSI (Fig-

ure 1), thus enhancing the final performance in terms of both noise reduction and structure preservation. More specifically, to take into account the non-local self-similarity in space, we group a set of similar cubics for each exemplar cubic as a 2D matrix, where each column represents the joint spectral-spatial information of one cubic, and enforce the spatial low-rank regularization on this set. Similarly, to utilize the spectral correlation, we form another 2D matrix where each column represents the joint local and non-local spatial information of one cubic, and use the spectral low-rank constraint on the constructed 2D matrix. These two low-rank regularizations are involved into a unified variational optimization model, which can be efficiently solved via an iterative numerical algorithm.

The remainder of this paper is organized as follows. Section 2 introduces the proposed spectral-spatial low-rank approximation HSI denoising method. Experimental results are reported in Section 3. We conclude the paper in Section 4.

2. PROPOSED ALGORITHM

Based on the additive Gaussian noise assumption, the HSI image degradation model can be mathematically formulated as: $\boldsymbol{y} = \boldsymbol{x}+\boldsymbol{n}$, where $\boldsymbol{y} \in \mathbb{R}^{MNB\times 1}$ is the the observed noisy HSI, $\boldsymbol{x}$ and $\boldsymbol{n}$ represents the desired clean HSI and noise, M, N, and B denotes the number of the rows, columns and bands, respectively. The goal of this work is to estimate the clean image $\boldsymbol{x}$ in presence of the degraded image $\boldsymbol{y}$ under noise variance σ^2 by solving the following constrained optimization problem:

$$\hat{\boldsymbol{x}} = \arg\min_{\boldsymbol{x}} P(\boldsymbol{x}) \quad subject\ to\ ||\boldsymbol{x}-\boldsymbol{y}||_2^2 \leq \sigma^2, \tag{1}$$

where $P(\bullet)$ is a regularization function on $\boldsymbol{x}$. In this work, we enforce two constraints on clean image. For one hand, the multiple spectral band can be well represented by the low-dimensional subspace, which relys on the fact that different spectral band exist information redundancy. For the other hand, the ubiquitous structural pattern recurrence phenomenon in natural image also exists in HSI, which motivates us to enforce the low-rank constraint to capture the underlying subspace structure of the similar cubics. By explicitly incorporating these low-rank priors into (1) with appropriate regularization parameters, the final problem can be formulated as the following unconstrained optimization problem:

$$\begin{aligned}\left\{\hat{\boldsymbol{x}}, \hat{\boldsymbol{P}}_i, \hat{\boldsymbol{Q}}_i\right\} = \arg\min_{\boldsymbol{x},\boldsymbol{P}_i,\boldsymbol{Q}_i} &||\boldsymbol{x}-\boldsymbol{y}||_2^2 \\ &+ \tau\sum\nolimits_i \left(||\tilde{\boldsymbol{R}}_i\boldsymbol{x}-\boldsymbol{P}_i||_F^2 + \alpha||\boldsymbol{P}_i||_*\right) \\ &+ \mu\sum\nolimits_i \left(||\bar{\boldsymbol{R}}_i\boldsymbol{x}-\boldsymbol{Q}_i||_F^2 + \beta||\boldsymbol{Q}_i||_*\right),\end{aligned} \tag{2}$$

where the HSI $\boldsymbol{x}$ is divided into overlapping cubic of size $P\times P\times B$, P is the length of spatial patch, $\tilde{\boldsymbol{R}}_i\boldsymbol{x} \in \mathbb{R}^{PPB\times K}$ indicates the formed matrix by the set of $K-1$ similar cubics for the vectorization of exemplar cubic $\boldsymbol{x}_i \in \mathbb{R}^{PPB\times 1}$. Similar to the spatial description, $\bar{\boldsymbol{R}}_i\boldsymbol{x} \in \mathbb{R}^{PPK\times B}$ means the formed matrix by the set of B bands for the vectorization of K spatial similar patches $\boldsymbol{x}_i \in \mathbb{R}^{PPK\times 1}$. $\boldsymbol{P}_i$ and $\boldsymbol{Q}_i$ is the desired clean low-rank matrix in spatial non-local and spectral subspace, respectively. $||\bullet||_*$ denotes the nuclear norm [11], τ, μ, α, and β are the corresponding regularization parameters. Our final model (2) is simple and easy to understand. The first term is the constraint of linear measurement. The second and the third terms are the low-rank prior enforced to preserve the structure relation in HSI. The proposed method can exploit simultaneously the spatial and spectral information, which facilitate the final denoising result.

2.1. Optimization

The proposed objective functional (2) can be efficiently solved by alternatively minimizing strategy with respect to the whole image $\boldsymbol{x}$ and low-rank matrix $\boldsymbol{P}_i$ and $\boldsymbol{Q}_i$ at per each location, so as to split the original problem into three simpler subproblems as follows:

$\boldsymbol{P}_i$ and $\boldsymbol{Q}_i$-subproblem: By ignoring terms independent of $\boldsymbol{P}_i$ and $\boldsymbol{Q}_i$in (2) respectively, we obtain following subproblems:

$$\begin{aligned}\hat{\boldsymbol{P}}_i &= \arg\min_{\boldsymbol{P}_i} ||\tilde{\boldsymbol{R}}_i\boldsymbol{x}-\boldsymbol{P}_i||_F^2 + \alpha||\boldsymbol{P}_i||_* \\ \hat{\boldsymbol{Q}}_i &= \arg\min_{\boldsymbol{Q}_i} ||\bar{\boldsymbol{R}}_i\boldsymbol{x}-\boldsymbol{Q}_i||_F^2 + \beta||\boldsymbol{Q}_i||_*.\end{aligned} \tag{3}$$

Equation (3) is the typical low-rank matrix approximation problem which has a closed-form solution and can be easily solved by the singular values thresholding algorithm [12]. In our implementation, we borrow the idea of the reweighting strategy to improve the performance.

$\boldsymbol{x}$-subproblem: After solving for each $\boldsymbol{P}_i$ and $\boldsymbol{Q}_i$, the latent HSI can be reconstructed by solving optimization problem:

$$\hat{\boldsymbol{x}} = \arg\min_{\boldsymbol{x}} ||\boldsymbol{x}-\boldsymbol{y}||_2^2 + \tau\sum\nolimits_i ||\tilde{\boldsymbol{R}}_i\boldsymbol{x}-\boldsymbol{P}_i||_F^2 + \mu\sum\nolimits_i ||\bar{\boldsymbol{R}}_i\boldsymbol{x}-\boldsymbol{Q}_i||_F^2. \tag{4}$$

Equation (4) is a quadratic optimization problem admitting a closed-form solution. The physical meaning of the solution is to calculate the overlapped pixels via aggregation, which can be computed in matrix element-wise division format efficiently. The algorithm procedure of the proposed method is summarized in **Algorithm 1**.

Algorithm 1 **S**pectral-**S**patial **L**ow-**R**ank **A**pproximation (**SSLRA**)

Require: Degraded image $\boldsymbol{y}$

1: **Initialize:**
2: • Set parameters τ, μ, α, and β;
3: • Initialize $\boldsymbol{x}^{(1)} = \boldsymbol{y}$;
4: **for** n=1:N **do**
5: Compute $\boldsymbol{P}_i$ and $\boldsymbol{Q}_i$ by solving Eq. (3);
6: Solve Eq. (4) for $\boldsymbol{x}^{k+1}$;
7: **end for**

Ensure: Clean Image $\boldsymbol{x}$.

Table 1. Mean quantitative results of differnent methods under several noise levels on Washington DC.

Sigma	Index	Methods								
		Noisy	BM3D	SDS	SSTV	LRMR	NMF	BM4D	TDL	SSLRA
10	PSNR	28.13	31.88	37.86	35.75	37.21	38.70	37.41	38.31	**39.38**
	SSIM	0.8348	0.9257	0.9787	0.9622	0.9748	0.9824	0.9780	0.9812	**0.9852**
	ERGAS	132.61	86.19	44.29	61.93	48.58	40.61	46.18	42.08	**36.97**
	SAM	0.2159	0.1068	0.0519	0.0869	0.0692	0.0507	0.0624	0.0542	**0.0479**
30	PSNR	18.59	26.24	31.18	30.70	29.64	31.99	30.92	31.40	**33.21**
	SSIM	0.4428	0.7568	0.9079	0.9010	0.8862	0.9241	0.9079	0.9192	**0.9448**
	ERGAS	397.85	165.22	95.98	100.44	116.23	86.20	97.65	92.92	**75.37**
	SAM	0.5497	0.1624	0.1189	0.1196	0.1489	0.0845	0.1081	0.0986	**0.0725**
50	PSNR	14.15	23.94	25.61	25.33	25.93	28.29	28.09	28.31	**30.24**
	SSIM	0.2465	0.6233	0.7507	0.7525	0.7851	0.8459	0.8310	0.8477	**0.8957**
	ERGAS	663.59	215.39	183.84	185.04	176.55	131.42	134.77	131.95	**105.77**
	SAM	0.7687	0.1918	0.2368	0.2395	0.2181	0.1185	0.1387	0.1213	**0.0915**

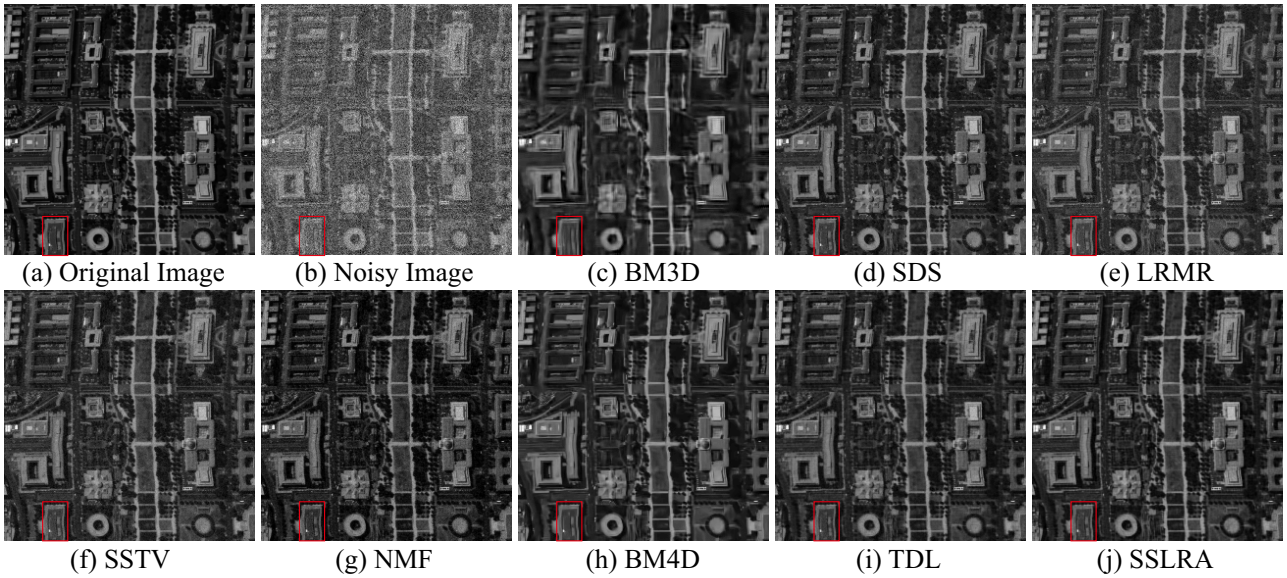

(a) Original Image (b) Noisy Image (c) BM3D (d) SDS (e) LRMR

(f) SSTV (g) NMF (h) BM4D (i) TDL (j) SSLRA

Fig. 2. Simulated random noise removal results at band 46 of Washington DC under noise level $\sigma = 30$.

3. EXPERIMENTAL RESULTS

We compared our SSLRA with state-of-the-art HSI denoising methods: BM3D [13], SDS [2], SSTV [5], LRMR [1], NMF [14], BM4D [10], TDL [7]. All the parameters are fine-tuned by default or following the rules in their papers to achieve the best performance.[1] The Matlab code of proposed method can be downloaded at the authors homepage.[2] The HSI Washington DC and AVIRIS are used as simulated and real data, respectively. The intensity of the data is normalized to [0, 255] beforehand. Four quantitative quality indices are employed, including peak signal-to-noise ratio (PSNR), structure similarity (SSIM), *erreur relative globale adimensionnelle de synthese* (ERGAS) and spectral angle map (SAM) to give an overall evaluation. The larger PSNR and SSIM values are, the better the restored images are. The smaller ERGAS and SAM values are, the better the restored images are.

Firstly, we test the proposed SSLRA method on Washington DC [3] for simulation results comparison (we choose an 256*256*31 sub-cubic [band30 - band60] as the input). Different degrees of zero-mean Gaussian noise (noise deviation 10, 30, 50) are added to each spectral band randomly. In Fig. 2, we can clearly see that the proposed method produces much cleaner result without any residual noise, meanwhile obtaining sharp texture and edge structure, compared with other competing methods. We also present the overall mean quantitative assessments of all competing methods under different noise level, as shown in Table 1. The best PSNR, SSIM, ERGAS and SAM values are highlighted in bold. The proposed SSLRA achieves the best performance in all cases. Moreover, with the increasing of noise level, the advantage of SSLRA over other methods becomes bigger.

[1] We downloaded all the codes from the authors' homepage.

[2] http://www.escience.cn/people/changyi/index.html

[3] https://engineering.purdue.edu/∼biehl/MultiSpec/hyperspectral.html

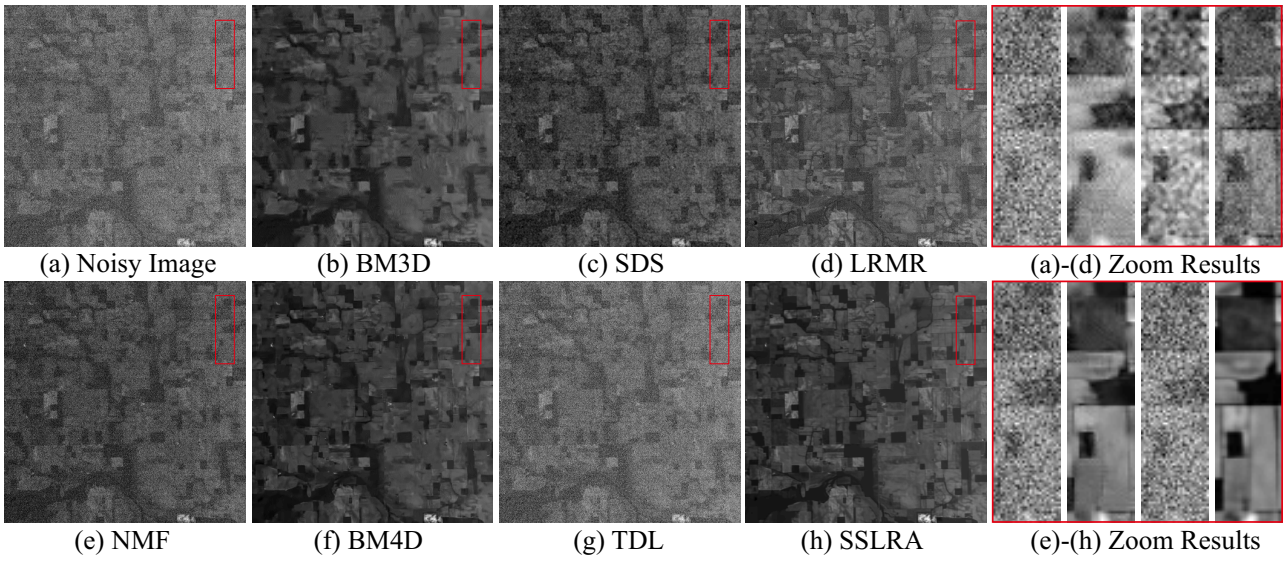

Fig. 3. Results comparison on AVIRIS under heavy noise level.

Then, we performed another real AVIRIS[4] denoising experiment to demonstrate the efficiency of our algorithm (we choose an 400*400*40 sub-cubic [band1 - band40] as the input), as shown in Fig. 3. It is shown that the proposed method clearly outperforms the compared methods with better visual appearance and less visual artifacts. From the demarcated window, the proposed SSLRA even restores abundant edge structure information from the overwhelming noise situation.

4. CONCLUSION

In this work, we propose to jointly utilize the spectral correlation and spatial non-local self-similarity property for HSI denoising. By introducing spectral low-rank constraint, the intrinsic low-dimensional spectral structure of HSI can be well depicted. Meanwhile, low-rank constraint on the spatial nonlocal cubics can reveal faithful subspace of the similar patterns. Within the unified spatial-spectral low-rank approximation model, our approach can remove the random noise more thoroughly with better structure preserving ability.

5. REFERENCES

[1] H. Zhang, W. He, L. Zhang, H. Shen, and Q. Yuan, "Hyperspectral image restoration using low-rank matrix recovery," *IEEE Trans. Geosci. Remote Sens.*, vol. 52, no. 8, pp. 4729–4743, Aug. 2014.

[2] A. Lam, I. Sato, and Y. Sato, "Denoising hyperspectral images using spectral domain statistics," in *Proc. IEEE Conf. ICPR*, 2012, pp. 477–480.

[3] Q. Yuan, L. Zhang, and H. Shen, "Hyperspectral image denoising employing a spectral–spatial adaptive total variation model," *IEEE Trans. Geosci. Remote Sens.*, vol. 50, no. 10, pp. 3660–3677, Oct. 2012.

[4] Y. Chang, L. Yan, H. Fang, and C. Luo, "Anisotropic spectral-spatial total variation model for multispectral remote sensing image destriping," *IEEE Trans. Image Process.*, vol. 24, no. 6, pp. 1852–1866, 2015.

[5] H. K. Aggarwal and A. Majumdar, "Hyperspectral image denoising using spatio-spectral total variation," *IEEE Geosci. Remote Sens. Lett.*, vol. 13, no. 3, pp. 1–5, 2016.

[6] X. Lu, Y. Wang, and Y. Yuan, "Graph-regularized low-rank representation for destriping of hyperspectral images," *IEEE Trans. Geosci. Remote Sens.*, vol. 51, no. 7, pp. 4009–4018, Jul. 2013.

[7] Y. Peng, D. Meng, Z. Xu, C. Gao, Y. Yang, and B. Zhang, "Decomposable nonlocal tensor dictionary learning for multispectral image denoising," in *Proc. IEEE Conf. CVPR*, 2014, pp. 2949–2956.

[8] Q. Xie, Q. Zhao, D. Meng, Z. Xu, S. Gu, W. Zuo, and L. Zhang, "Multispectral images denoising by intrinsic tensor sparsity regularization," in *Proc. IEEE Conf. CVPR*, 2016, pp. 1692–1700.

[9] W. Dong, G. Li, G. Shi, X. Li, and Y. Ma, "Low-rank tensor approximation with laplacian scale mixture modeling for multiframe image denoising," in *Proc. IEEE Conf. ICCV*, 2015, pp. 442–449.

[10] M. Maggioni, V. Katkovnik, K. Egiazarian, and A. Foi, "Nonlocal transform-domain filter for volumetric data denoising and reconstruction," *IEEE Trans. Image Process.*, vol. 22, no. 1, pp. 119–33, 2012.

[11] Y. Chang, L. Yan, T. Wu, and S. Zhong, "Remote sensing image stripe noise removal: from image decomposition perspective," *IEEE Trans. Geosci. Remote Sens.*, vol. 54, no. 12, pp. 7018–7031, 2016.

[12] J.-F. Cai, E. J. Candès, and Z. Shen, "A singular value thresholding algorithm for matrix completion," *SIAM J. on Optim.*, vol. 20, no. 4, pp. 1956–1982, Jan. 2010.

[13] K. Dabov, A. Foi, V. Katkovnik, and K. Egiazarian, "Image denoising by sparse 3-d transform-domain collaborative filtering," *IEEE Trans. Image Process.*, vol. 16, no. 8, pp. 2080–2095, Aug. 2007.

[14] M. Ye, Y. Qian, and J. Zhou, "Multitask sparse nonnegative matrix factorization for joint spectral–spatial hyperspectral imagery denoising," *IEEE Trans. Geosci. Remote Sens.*, vol. 53, no. 5, pp. 2621–2639, 2015.

[4] http://aviris.jpl.nasa.gov/